Nuclear Instruments and Methods in Physics Research B 379 (2016) 62–68

Contents lists available at ScienceDirect

Nuclear Instruments and Methods in Physics Research B

journal homepage: www.elsevier.com/locate/nimb

Thermoluminescence studies of γ-irradiated ZnO:Mg^{2+} nanoparticles

N. Pushpa [a], M.K. Kokila [a,*], K.R. Nagabhushana [b]

[a] Department of Physics, Bangalore University, Bangalore 560 056, India
[b] Department of Physics (S & H), PES University, Bangalore 560 085, India

ARTICLE INFO

Article history:
Received 12 November 2015
Received in revised form 19 March 2016
Accepted 20 April 2016
Available online 10 May 2016

Keywords:
ZnO nanoparticles
Gamma rays
Photoluminescence
Thermoluminescence

ABSTRACT

Pure and Mg^{2+} doped ZnO nanoparticles are synthesized by solution combustion method. X-ray diffraction studies of the samples confirm hexagonal phase. Crystallite size is calculated using Scherer formula and found to be ~30 nm for undoped ZnO and 34–38 nm for Mg^{2+} doped ZnO. A broad PL emission in the range 400–600 nm with peaks at 400, 450, 468, 483, 492, 517, 553 nm are observed in both pure and Mg^{2+} doped nanoparticles. Near band edge emission of ZnO is observed at 400 nm. The broad band emissions are due to surface defects. PL emission intensity is found to increase with Mg^{2+} concentration up to 1.5 mol% and then decreases due to concentration quenching. Samples are irradiated with γ-rays in a dose range 0.05–8 kGy. Gamma irradiation doesn't affect PL properties. Undoped samples exhibit unstructured low intense TL glow with peak at 720 K. Whereas Mg^{2+} doped samples exhibit well structured TL glow curves with peak at ~618 K. TL glow peak intensity of Mg^{2+} doped samples increases with Mg^{2+} concentration up to 2 mol%, thereafter decreases. TL curves of Mg^{2+} (2 mol%) doped ZnO exhibit two glows, a high intense peak at 618 K and a weak one with peak at ~485 K. TL intensity of Mg^{2+} (2 mol%) doped ZnO samples increases with gamma dose up to 1 kGy and then decreases. Kinetic parameters of TL glows are calculated by deconvolution technique. Activation energy and frequency factor are found to be 1.5 eV and 3.38×10^{11} s^{-1} respectively.

1. Introduction

Zinc oxide (ZnO) nanostructures have been greatly influenced the researchers due to its potential applications in optoelectronics, sensors, transducers and biomedical field [1,2]. ZnO is a direct band gap semiconductor with a band gap of 3.37 eV at room temperature. It exhibit luminescence due to the presence of intrinsic defects [3]. Emission related to defects depends on microstructure, defect types and their concentration resulting in ultraviolet to red region [4,5]. Doping of impurities provide a way to modify the properties of nanostructures by changing their compositions [6]. Although attempts are made to investigate an underlying mechanism that controls the properties of doped material, knowledge is still limited. ZnO doped with Mg^{2+} permits band gap narrowing [6,7] and wavelength tunability [8] to blue or even green light spectra range by creating barrier layers, which will facilitate radiative recombination by carrier confinement [9,10].

Thermoluminescence (TL) is a powerful tool to study luminescence centers responsible for the emission in materials. TL technique is used to measure the radiation dose absorbed by material. Numbers of commercial TL dosimeters (TLD) are more often used for clinical, environmental and personal dosimetry applications. However, these TLD's cannot be used for high dose applications because TL intensity saturates due to the overlapping of ionized zones. Nanomaterials have potential applications in high dose TL dosimetry. Hence there is a substantial scope of research for development of new nanophosphor with enhanced TL dosimetric properties [11].

Numbers of chemical methods have been applied to synthesize ZnO nanostructures viz hydrothermal [12], precipitation [13], sol–gel [14], solution combustion and thermal decomposition [15,8] techniques, etc. Among these, combustion synthesis provides a molecular level mixing and high degree of homogeneity, short reaction time that leads to reduction in crystallization temperature and prevents from segregation during heating. In the present studies, undoped and Mg^{2+} doped zinc oxide nanoparticles are synthesized using solution combustion technique and the effect of Mg^{2+} doping on luminescence properties are investigated. Also, TL properties of ZnO:Mg^{2+} nanophosphor are studied for its use in high radiation dose.

* Corresponding author.
E-mail address: drmkkokila@gmail.com (M.K. Kokila).

http://dx.doi.org/10.1016/j.nimb.2016.04.042
0168-583X/

2. Experimental

2.1. Synthesis

Pure and Mg^{2+} doped ZnO nanoparticles are synthesized by solution combustion method. The starting materials are zinc nitrate (Sigma Aldrich), urea (Merck chemicals, India) and magnesium nitrate (Sigma Aldrich). The experiment is performed by dissolving stoichiometric amount of above reagents together in a minimum amount of double distilled water. ZnO nanopowders are prepared with different concentrations of Mg^{2+} ions (0.1, 0.5, 1.0, 2.0 and 3.0 mol%). The detailed procedure of combustion synthesis is reported elsewhere [16]. The obtained samples are annealed at 500 °C for 3 h in muffle furnace.

2.2. Characterization

Phase purity of the nanoparticles is characterized by powder X-ray diffraction (XRD) using Rigaku Miniflex II diffractometer with Cu Kα (λ = 1.541 Å) radiation. Surface morphology of the powders is examined by scanning electron microscope (SEM) (Hitachi S-300N model). Diffused reflectance is recorded using Shimazdu (UV-1800). Photoluminescence (PL) measurements are performed using Hitachi Spectroflourometer (Model F-2700) equipped with 150 W Xenon lamp as an excitation source. For TL measurements, 40 mg of nanophosphor are exposed to γ-rays (^{60}Co) in a dose range 0.05–8.00 kGy. TL measurements are carried out on a TL Reader (model: TL1009I; Nucleonix Systems Pvt Ltd, Hyderabad, India) in the temperature range 325–750 K.

3. Results and discussion

3.1. X-ray diffraction

XRD patterns of undoped and Mg doped nanostructures are shown in Fig. 1. Sharp diffraction peaks manifest that undoped and Mg^{2+} nanostructures show high crystallinity. The diffraction peaks are corresponding to (100), (002), (101), (102), (110), (103), (112) and (200) planes are in good agreement with wurtzite hexagonal crystalline phase (JCPDS: 36-1451). Thus, obtained ZnO nanophosphor having phase purity because Mg^{2+} substitution did not alter the wurtzite structure. Crystallite size is calculated by Scherer formula and found to be ~30 nm for undoped ZnO and 34–38 nm for Mg^{2+} doped ZnO. Also, lattice parameters *a* and *c* are calculated and found to be 3.338 ± 0.001 Å and 5.239 ± 0.003 Å, respectively.

3.2. Scanning electron microscopy

SEM image of pure and Mg^{2+} (3 mol%) ZnO are shown in Fig. 2. It is evident that ZnO nanoparticles are spherical in shape with different sizes. Whereas morphology of Mg^{2+} (3 mol%) ZnO shows aggregated nanoparticles having higher diameters. It is well known that morphology of the prepared powders is strongly dependent on heat and gases liberated during combustion reaction. Hence, voids and pores are present in the sample.

3.3. Diffuse reflectance spectroscopy

Diffused reflectance spectra of undoped and Mg doped ZnO nanoparticles are shown in Fig. 3. All the samples show diffused reflectance at 380–400 nm. Band gap of undoped and Mg^{2+} doped ZnO particles is calculated using Kubelka Munk equation given below [17]

$$\frac{k}{s} = \frac{(1-R)^2}{2R} \quad (1)$$

where *R* is reflectance, *k* is absorption coefficient and s is scattering coefficient. Band gap (*Eg*) is estimated from the graph of $[(k/s)h\nu]^2$ versus $h\nu$, by extrapolating graph to the *X*-axis (shown as inset). Eg of undoped ZnO is found to be 3.24 eV. Eg of ZnO decreases with increase in Mg^{2+} concentration. 2 mol% Mg^{2+} doped ZnO is found to be *Eg* of 2.95 eV. This confirms the presence of Mg content in host.

3.4. Photoluminescence

PL is an effective way to study electronic structure, defects, optical and photochemical properties of semiconductor materials. PL spectra of the nanoparticles are measured at an excitation wavelength of 325 nm using Xenon lamp. PL emission spectra of pure and ZnO:Mg^{2+} nanoparticles (un irradiated) are shown in Fig. 4. It is observed that all the samples show violet emission

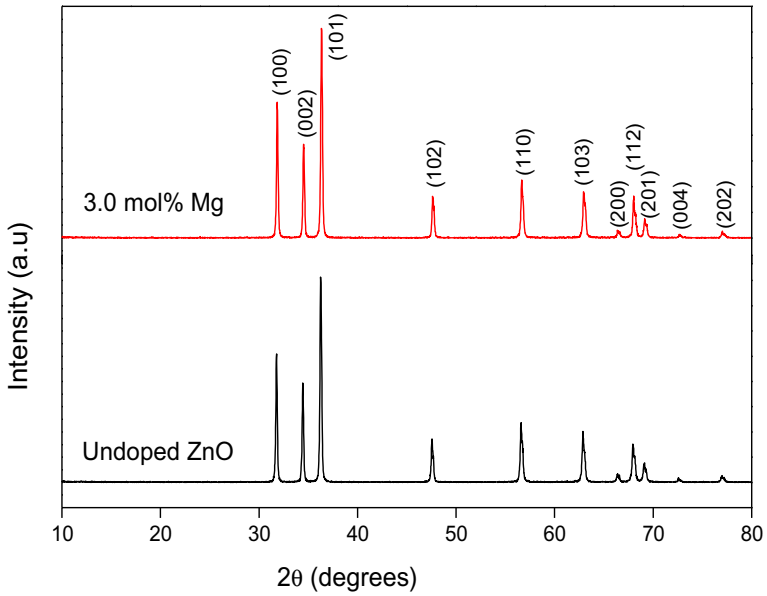

Fig. 1. XRD studies of pure and Mg^{2+} doped ZnO nanoparticles.

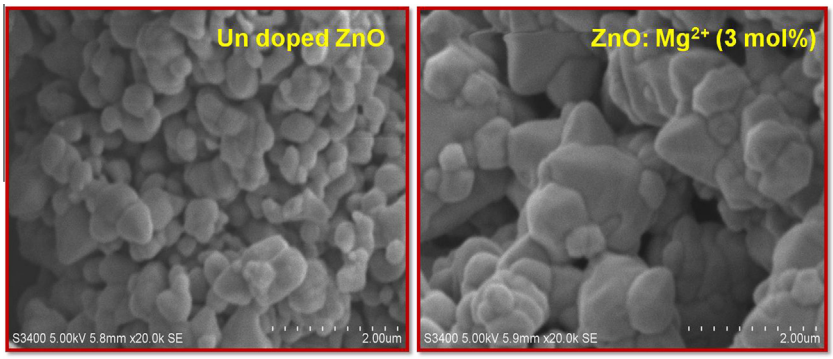

Fig. 2. SEM micrograph of undoped and Mg^{2+} (3 mol%) doped ZnO.

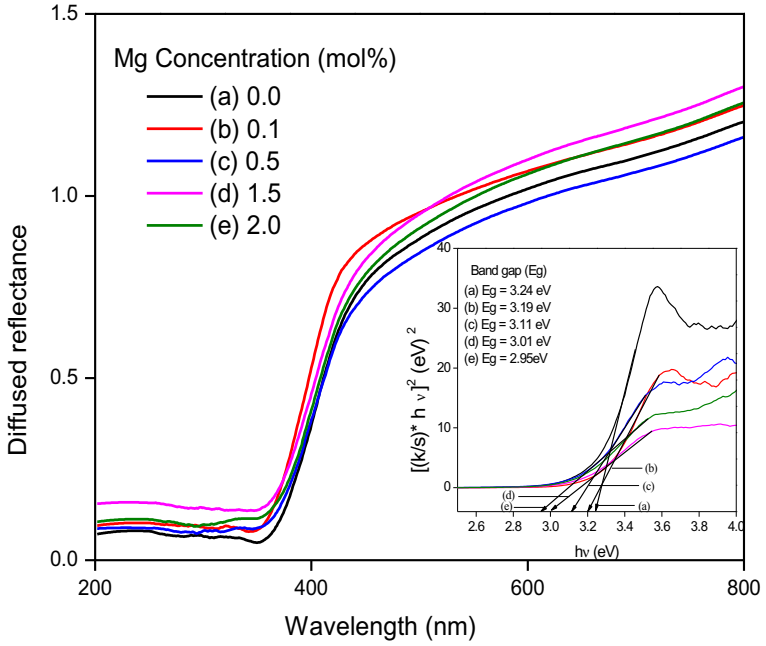

Fig. 3. Diffused reflectance spectra of undoped and Mg^{2+} doped ZnO nanoparticles.

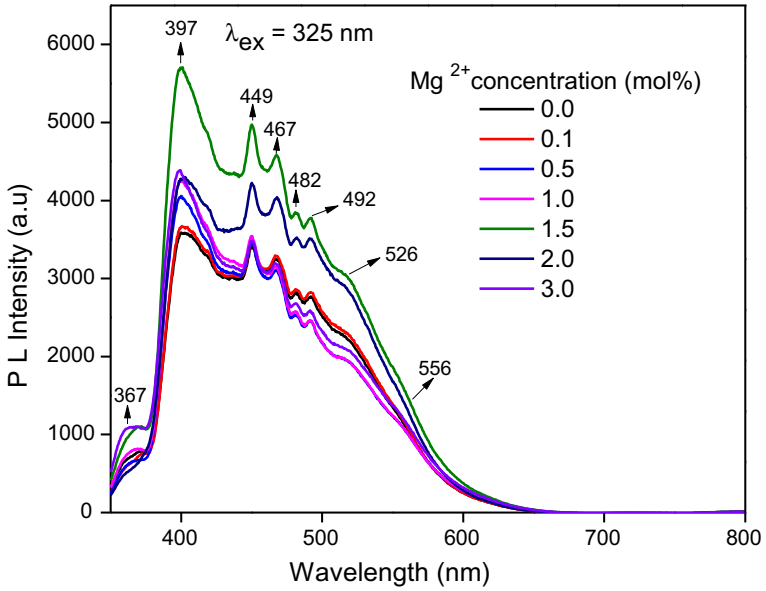

Fig. 4. PL spectra of ZnO:Mg^{2+} nanoparticles.

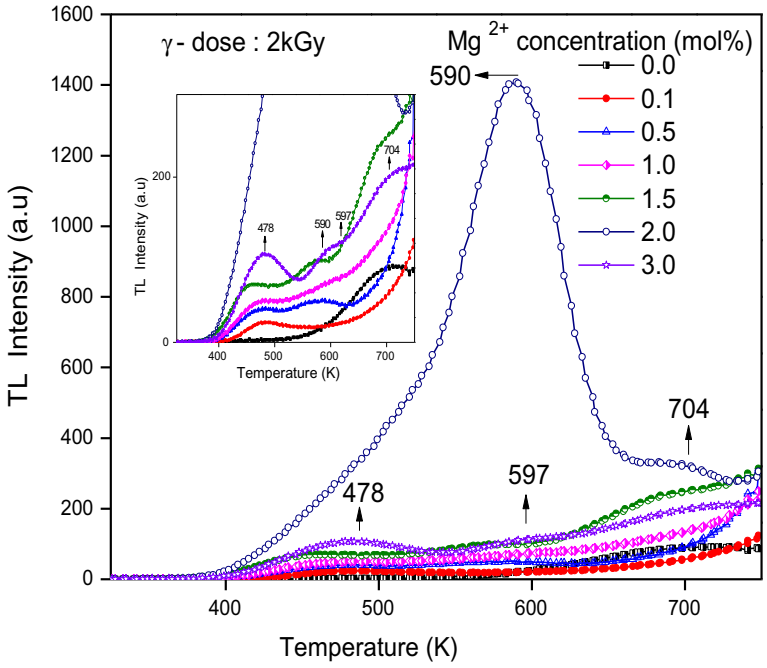

Fig. 5. TL glow curves of ZnO:Mg^{2+} nanoparticles irradiated with 2 kGy gamma rays.

peaks at 367, 400 nm, blue emission peaks at 468, 483, 492 nm and weak green emission peaks at 517 and 553 nm. The violet emission corresponds to near band edge emission of wide band gap of ZnO due to annihilation of exciton [18]. The broad blue band emissions are possibly due to surface defects such as oxygen vacancies (V_O) and Zinc interstitials (Zn_i). The green luminescence is attributed to radiative recombination of photo generated holes in valence band with electrons in singly occupied oxygen vacancies [18–21]. It is observed that intensity of PL emission increases with Mg^{2+} concentration up to 1.5 mol% and then decreases. This is due to concentration quenching. PL of gamma irradiated samples is also studied. But gamma irradiation doesn't affected PL property of undoped and Mg doped nanoparticles.

3.5. Thermoluminescence

3.5.1. TL glow curve analysis

TL glow curves of ZnO:Mg^{2+} samples irradiated with gamma rays for a dose of 2 kGy are shown in Fig. 5. TL glow curves are recorded at an heating rate of 5 K s^{-1}. Undoped samples exhibit unstructured low intense TL glow with peak at 720 K. Whereas Mg^{2+} doped samples exhibit well structured TL glow curves with peak at ~618 K. This is due to the fact that Mg^{2+} doping in the material could help in generating more number of electron/hole traps and luminescent centers responsible for TL. Variation of TL glow peak intensity with Mg^{2+} concentration is shown in Fig. 6. Maximum TL intensity is observed for the concentration of 2 mol%.

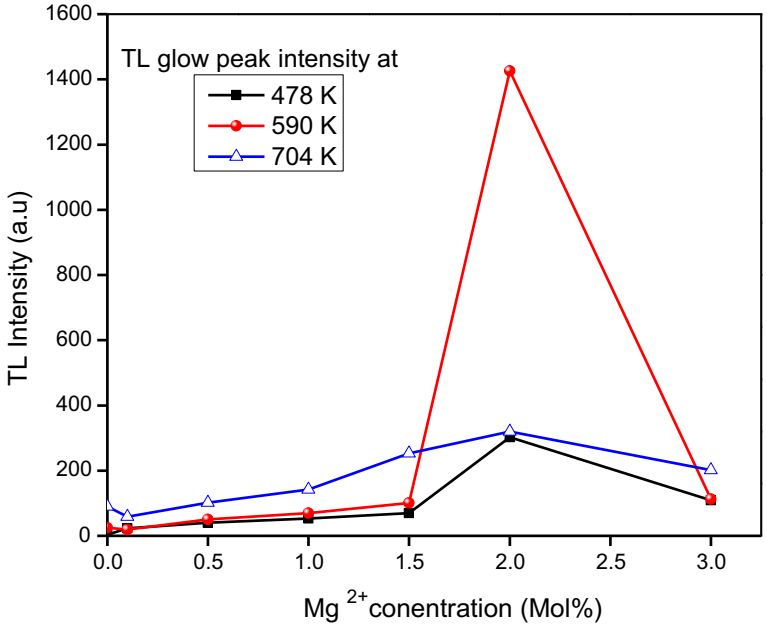

Fig. 6. Variation of TL glow peak intensity and glow peak temperature with Mg^{2+} concentration (mol%).

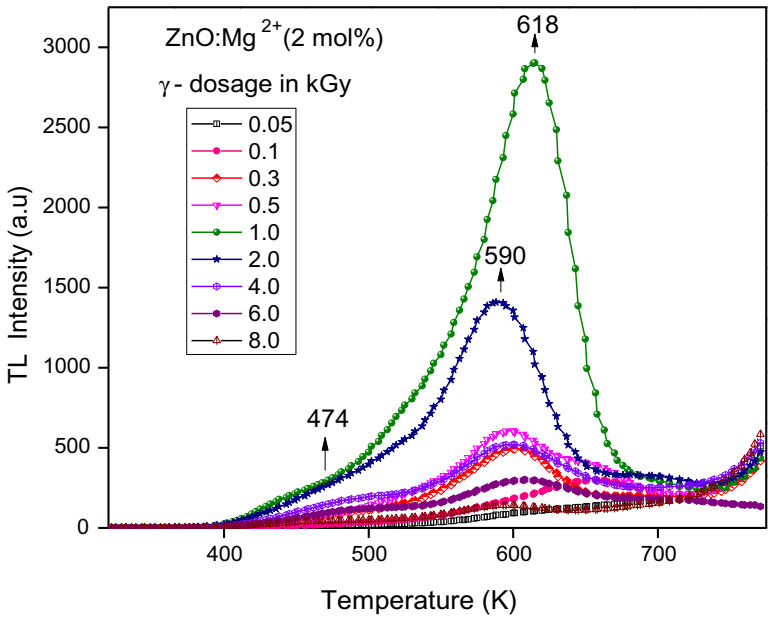

Fig. 7. TL glow curves of gamma irradiated Mg^{2+} (2 mol%) doped ZnO.

Hence this sample is exposed to gamma rays for various doses to study its TL properties. TL glow curves of ZnO:Mg^{2+} (2 mol%) exposed to gamma rays for various dose is shown in Fig. 7. TL glow curves exhibit two peaks, high intense one at 618 K and a weak one at ~485 K for all the dose [22,15]. It is known that, low temperature TL glows are due to shallow traps and high temperature TL glows are due to deep traps. Intrinsic defects have been considered as possible charge donor sources in ZnO. They are the oxygen vacancy (V_O) and zinc interstitial (Zn_i). It is usually accepted that zinc interstitial is a shallow donor. It is reported that, V_O has relatively deep energy levels [23]. Fig. 8 shows variation of TL glow peak intensity with γ-dose. It is observed that, TL intensity increases linearly up to 1 kGy and thereafter decreases. The increase in TL intensity may be due to creation of defects centers such as F-centers and hole centers and decrease in TL intensity might be attributed to overlapping of ionized zones [24]. Further with increase of gamma dose, the glow peaks are well structured and temperature maxima of TL glows are shifted towards higher temperature side. A shift of about 20 K is observed.

3.5.2. Effect of heating rate on TL glow curves

Effect of different heating rate on TL glow curves is investigated for ZnO:Mg^{2+} (1 mol%) exposed to γ-dose of 4 kGy and is shown in Fig. 9. It is found that, TL glow peak intensity and area under the curve increases with heating rate up to 5 K s^{-1} thereafter it decreases. The decrease in TL intensity with increase in heating rate is due to thermal quenching. Further, glow peak temperature shifts towards higher temperature side with heating rate. The glow peak maximum (T_m) is shifted from 590 to 612 K with increase of heating rate from 1 to 7 K s^{-1}.

3.5.3. TL Kinetic parameters

Characteristics of dosimeters used in TL process are related to kinetic parameters and these parameters qualitatively describe

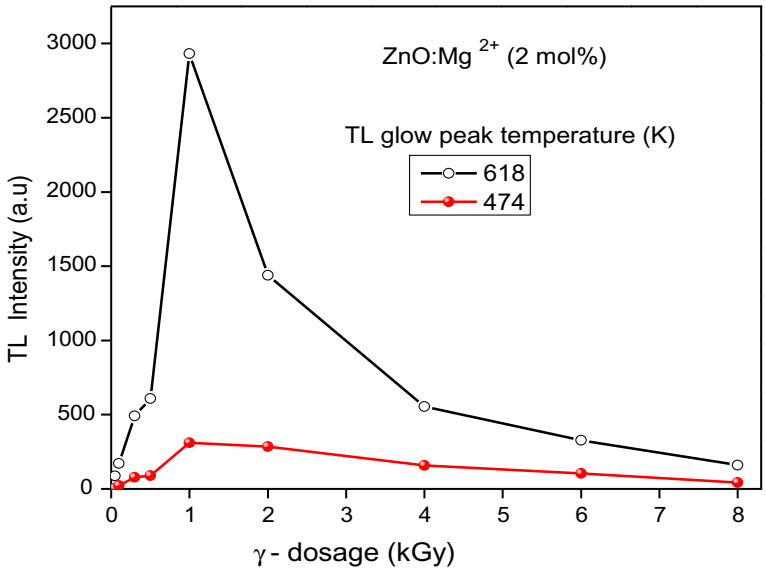

Fig. 8. Variation of TL glow peak intensity with γ-dose in ZnO:Mg^{2+} (2 mol%) nanoparticles.

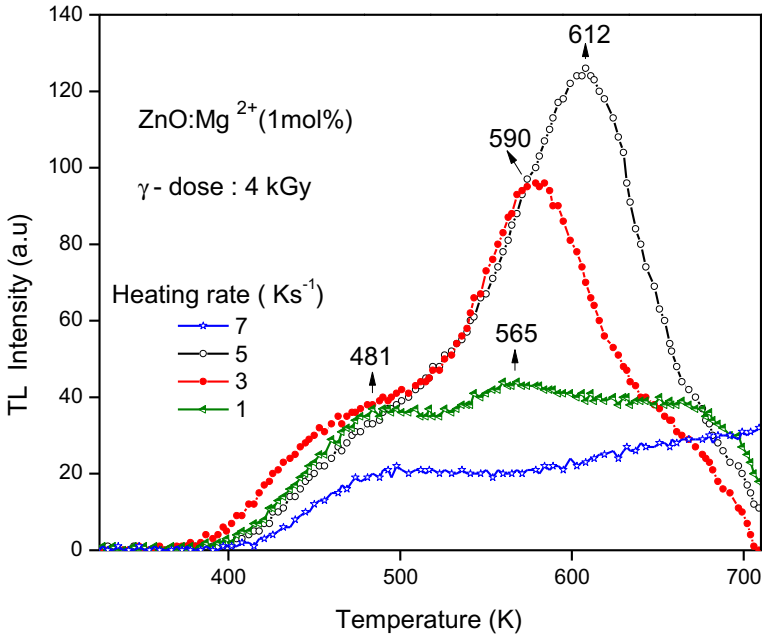

Fig. 9. TL glow curves of for ZnO:Mg^{2+} (1 mol%) nanoparticles recorded at different heating rates.

the trapping/emitting centers. Detailed studies of the kinetic parameters provide valuable information regarding the TL mechanism responsible for dosimetric applications. A reliable dosimetric study of a TL material should be based on a good knowledge of the kinetic parameters. TL glow curve is deconvoluted using a computerized curve de convolution analysis (GCD) [25]. Kitis et al. [26] suggested the equation for general order kinetics which is used for glow curve de convolution

$$I(t) = I_m b^{\frac{b}{b-1}} \left(\frac{E}{kT}\frac{T-T_m}{T_m}\right) \left[(b-1)(1-\Delta)\frac{T^2}{T_m^2}\exp\left(\frac{E}{kT}\frac{T-T_m}{T_m}+Z_m\right)\right]^{-\frac{b}{b-1}} \quad (2)$$

with $\Delta = 2kT/E$, $\Delta_m = 2kT_m/E$

$$Z_m = 1 + (b-1)\Delta_m$$

where 'k' is Boltzmann constant (8.6×10^{-5} eV K^{-1}), I_m is the glow peak intensity, β is the linear heating rate (5 K s^{-1}) and b is the order of kinetics and T_m is glow peak temperature. The Software Package Microsoft Excel has been used for curve fitting [25]. For the fitting, one has to input the initial, arbitrary but meaningful values for the parameters I_m, T_m, E and b for each single glow peak. When the curve fitting is completed, it gives the net values of I_m, T_m, E and b. In addition, the frequency factor and figure of merit (FOM) values are determined using expressions given below

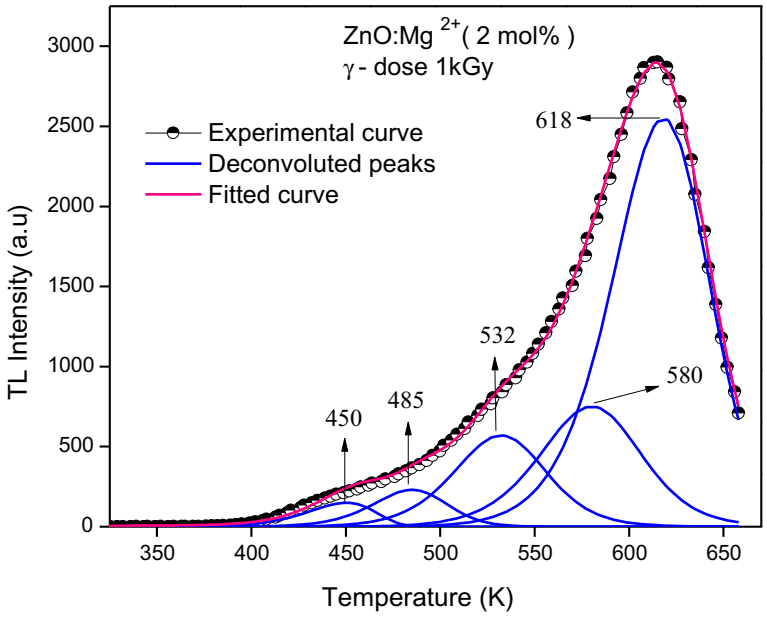

Fig. 10. Deconvoluted glow curves of ZnO:Mg^{2+} (2 mol%).

Table 1
Kinetic parameters of ZnO:Mg^{2+} (1 mol%) nanoparticles for the γ-dose 2 kGy.

γ-dose	T_m (K)	b	E_{av} (eV)	s (s^{-1})	FOM (%)
2 kGy	450	1.0	0.95	1.18×10^{10}	
	485	1.4	1.20	8.38×10^{11}	
	532	1.6	1.25	1.70×10^{11}	1.85
	580	1.6	1.35	1.20×10^{11}	
	618	1.4	1.5	3.78×10^{11}	

$$\frac{\beta E}{kT_m^2} = s\ \exp\frac{-E}{KT_m}[1+(b-1)\Delta_m] \tag{3}$$

$$\mathrm{FOM} = \frac{\sum |\mathrm{TL_{exp}} - \mathrm{TL_{the}}|}{\sum \mathrm{TL_{the}}} \tag{4}$$

Here TL_{exp} and TL_{the} represent TL intensity of experimental and theoretical glow curves respectively. The fits are considered to be good when the FOM values are below 5%. TL glow curve deconvolutions of synthesized nanostructures are performed. Undoped samples exhibit unstructured low intense TL glow peak. This TL glow is deconvoluted into four peaks. Mg ion doped samples exhibit well structured TL glow curves. Experimental TL glow curves of all the samples doped with Mg are deconvoluted into six TL peaks. Fig. 10 shows deconvoluted TL glow curves of ZnO doped with 2 mol% Mg^{2+} irradiated with γ-dose of 1 kGy. The calculated kinetic parameters are given in Table 1. Deconvoluted TL glow exhibit peaks at 450,585, 532, 580, 618 K. It is observed that activation energy of deconvoluted peaks increases with increase of glow peak temperature. This indicates that each glow peak has different trap levels in the band gap of a material.

4. Conclusions

Combustion synthesized ZnO exhibits hexagonal wurtzite structure. Crystallite size is found to be in the range 30–38 nm. ZnO nanoparticles are in spherical in shape and ZnO:Mg^{2+} particles are agglomerated. PL studies show that enhancement of intensity upon Mg^{2+} doping up to 1.5 mol%. TL studies of γ-irradiated ZnO:Mg^{2+} nanoparticles exhibits two glow peaks, high intense peak at 618 K and weak one with peak at ~485 K. TL intensity increases linearly with increase in γ-dose from 0.05 to 1 kGy. Hence, this material may be useful for TL dosimetry applications in the dose range 0.05–1 kGy.

Acknowledgement

The Authors (PN & MKK) acknowledge Department of Atomic Energy and Board of Research in Nuclear Science (DAE–BRNS), BARC, India for providing financial support to carry out this research work (project No. 2011/37P/18/BRNS).

References

[1] S. Pearton, Prog. Mater Sci. 50 (2005) 293–340, http://dx.doi.org/10.1016/j.pmatsci.2004.04.001.
[2] U. Ozgur, Ya.I. Alivov, C. Liu, A. Teke, M.A. Reshchikov, S. Dogan, Appl. Phys. 98 (2005) 1–3, http://dx.doi.org/10.1063/1.1992666.
[3] M.D. McCluskey, S.J. Jokela, Appl. Phys. 106 (2009) 071101, http://dx.doi.org/10.1063/1.3216464.
[4] A. Janotti, C.G. Van De Walle, Phys. Rev. B Condens. Matter Mater. Phys. 76 (2007) 1–22, http://dx.doi.org/10.1103/PhysRevB.76.165202.
[5] M.K. Kavitha, K.B. Jinesh, R. Philip, P. Gopinath, H. John, Phys. Chem. Chem. Phys. 16 (2014) 25093–25100, http://dx.doi.org/10.1039/C4CP03847A.
[6] J. Singh, P. Kumar, K.N. Hui, J. Jung, R.S. Tiwari, O.N. Srivasatva, RSC Adv. 3 (2013) 5465, http://dx.doi.org/10.1039/c3ra23046e.
[7] J. Zhang, F. Pan, W. Hao, T. Wang, Mater. Sci. Eng. B Solid State Mater. Adv. Technol. 129 (2006) 93–95, http://dx.doi.org/10.1016/j.mseb.2005.12.028.
[8] V. Etacheri, R. Roshan, V. Kumar, ACS Appl. Mater. Interfaces 4 (2012) 2717–2725, http://dx.doi.org/10.1021/am300359h.
[9] J. Singh, P. Kumar, K.S. Hui, K.N. Hui, K. Ramam, R.S. Tiwari, O.N. Srivasatva, CrystEngComm (2012) 5898–5904, http://dx.doi.org/10.1039/c2ce06650e.
[10] F.K. Shan, B.I. Kim, G.X. Liu, Z.F. Liu, J.Y. Sohn, J. Appl. Phys. (2004) 4772–4776, http://dx.doi.org/10.1063/1.1690091.
[11] S.P. Lochab, D. Kanjilal, N. Salah, S.S. Habib, Jyoti Lochab, R. Ranjan, V.E. Aloeynikov, A.A. Rupasov, A. Pandey, J. Appl. Phys. 104 (2008) 033520–033523, http://dx.doi.org/10.1063/1.2955459.
[12] W. Bai, K. Yu, Q. Zhang, F. Xu, D. Peng, Z. Zhu, Mater. Lett. 61 (2007) 3469–3472, http://dx.doi.org/10.1016/j.matlet.2006.11.103.
[13] B. Li, Y. Wang, Superlattices Microstruct. (2010) 1–9, http://dx.doi.org/10.1016/j.spmi.2010.02.005.
[14] N. Kumar, R. Kaur, R.M. Mehra, J. Lumin. 126 (2007) 784–788, http://dx.doi.org/10.1016/j.jlumin.2006.11.012.
[15] A.J. Reddy, M.K. Kokila, H. Nagabhushana, J.L. Rao, C. Shivakumara, B.M. Nagabhushana, Spectrochim. Acta Part A Mol. Biomol. Spectrosc. 81 (2011) 53–58, http://dx.doi.org/10.1016/j.saa.2011.05.043.
[16] S.T. Aruna, A.S. Mukasyan, Curr. Opin. Solid State Mater. Sci. 12 (2008) 44–50, http://dx.doi.org/10.1016/j.cossms.2008.12.002.
[17] C. Aydın, M.S.A. El-sadek, K. Zheng, I.S. Yahia, F. Yakuphanoglu, Opt. Laser Technol. 48 (2013) 447–452, http://dx.doi.org/10.1016/j.optlastec.2012.11.004.
[18] Y. Wang, X. Zhao, L. Duan, F. Wang, H. Niu, W. Guo, Mater. Sci. Semicond. Process. 29 (2015) 372–379, http://dx.doi.org/10.1016/j.mssp.2014.07.034.
[19] L. Duan, X. Zhao, Z. Zheng, J. Phys. Chem. Solids 76 (2014) 88–93, http://dx.doi.org/10.1016/j.jpcs.2014.07.003.
[20] A.N. Mallika, A. Ramachandra Reddy, K. Sowri Babu, C. Sujatha, K. Venugopal Reddy, Opt. Mater. 36 (2014) 879–884, http://dx.doi.org/10.1016/j.optmat.2013.12.015.
[21] Y. Wu, J. Yun, L. Wang, X. Yang, Cryst. Res. Technol. 48 (2013) 145–152, http://dx.doi.org/10.1002/crat.201200438.
[22] C. Cruz-Vázquez, R. Bernal, Radiat. Eff. Defects Solids (2014) 380–387, http://dx.doi.org/10.1080/10420150.2014.905943.
[23] A. Janotti, C.G. Van De Walle, Phys. Rev. B 76 (2007) 1–22, http://dx.doi.org/10.1103/PhysRevB.76.165202.
[24] M.S. Kulkarni, K.P. Muthe, N.S. Rawat, D.R. Mishra, M.B. Kakade, S. Ramanathan, Radiat. Meas. 43 (2008) 492–496, http://dx.doi.org/10.1016/j.radmeas.2007.10.039.
[25] D. Afouxenidis, G.S. Polymeris, N.C. Tsirliganis, G. Kitis, Radiat. Prot. Dosim. 149 (2012) 363–370, http://dx.doi.org/10.1093/rpd/ncr315.
[26] G. Kitis, J.M. Gomez-Ros, J.W.N. Tuyn, J. Phys. D Appl. Phys. 31 (1998) 2636–2641, http://dx.doi.org/10.1088/0022-3727/31/19/037.